

*SENSITIVITY STUDIES USING A CLIMATE THERMODYNAMIC  
MODEL, WITH PARTICULAR REFERENCE  
TO THE EFFECT OF CHANGING THE SOLAR CONSTANT*

J. ADEM\*

*Received Sept. 5, 1980*

RESUMEN

El modelo termodinámico del autor se aplica para estudiar el efecto de cambios en la constante solar en el clima terrestre. Se usan pasos de tiempo de un mes que toman en cuenta las variaciones estacionales de la insolación. Las extensiones horizontales de una cubierta de nubes y otra de hielo y nieve se incluyen como variables. Después de 4 ó 5 años de integración de las ecuaciones, se obtiene la solución estacionaria que se usa para evaluar el efecto de los cambios en la constante solar.

Según los cálculos del modelo, una disminución de 2 por ciento en la constante solar produce anomalías negativas en la superficie que son mayores en julio que en enero. El efecto de la distribución de continentes y océanos aparece en la solución, especialmente en julio. Las anomalías mayores se obtienen en julio sobre los continentes y alcanzan valores de -5.1 grados Celsius en una latitud de 30° en América y de -6.0 grados en una latitud de 20° en Asia. Los valores zonalmente promediados de la disminución de la temperatura en la superficie debida a una disminución en la constante solar de 2 por ciento, en julio varía de 2.3° en latitudes bajas a 1.0° en latitudes altas, y en enero de 1.7° en latitudes bajas a 0.5° en latitudes altas. Además, se demuestra que una disminución de 2 ó 4 por ciento en la constante solar no produce un aumento significativo en la extensión de la cubierta de hielo y nieve. Las anomalías en la cubierta de nubes que aparecen debido a la disminución en la constante solar, tienen una influencia fuerte en la disminución de la temperatura en la superficie, especialmente en latitudes bajas. Las soluciones muestran que es esencial en todo modelo climático incluir la cubierta de nubes como variable.

El promedio anual calculado del cambio de la temperatura en la superficie debido a una disminución de uno por ciento es igual a 0.7° C. Se hace una comparación de este valor con los obtenidos por otros autores.

\* *Centro de Ciencias de la Atmósfera y Facultad de Ciencias, Universidad Nacional Autónoma de México, México 20, D.F.*

## ABSTRACT

The author's thermodynamic model is applied to study the effect of changes in the solar constant on the climate of the Earth. Time steps of one month are used which take into account seasonal variations of the insolation. The horizontal extent of snow-ice and cloud covers are included as variables. After 4 or 5 years of integration the solution reaches a steady state, which is the one used to evaluate the effect of the changes in the solar constant.

According to the computations, a decrease of 2 percent in the present solar constant produces negative anomalies in the surface temperature, which are stronger in July than in January. The effect of the distribution of continents and oceans appears in the solution, especially in July. The largest anomalies are obtained in July over the continents reaching values of -5.1 degrees Celsius at latitude  $30^{\circ}$  over America and -6.0 degrees at latitude  $20^{\circ}$  over Asia. The zonally averaged values of the decrease of surface temperature due to a decrease of 2 percent in the solar constant, in July varying from  $2.3^{\circ}$  C in lower latitudes to  $1.0^{\circ}$  C in higher latitudes, and in January varying from  $1.7^{\circ}$  in lower latitudes to  $0.5^{\circ}$  C in higher latitudes. Furthermore, it is shown that a decrease of 2 or 4 percent in the solar constant does not produce a substantial increase in the position of the snow and ice boundary. The anomalies in the cloud cover, that appear due to the decrease in the solar constant, have a strong influence in the surface temperature decrease especially in lower latitudes. The solutions show that it is essential in any climate model to include cloudiness as a variable.

The computed annual average value of the change in the surface temperature due to a decrease of one percent is equal to  $0.7^{\circ}$  C. A comparison with the results obtained by other authors and models is carried out.

## INTRODUCTION

The evaluation of the sensitivity of climate to climatic forcing has been one of the important applications of mathematical models, and the number of papers that have been published on the subject using all types of models, from the simplest to the most sophisticated ones, is very large, so that comparison of results using the same change in climate forcing, but different model has become indispensable, and has been useful to understand the importance of physical processes as well as of the modelling approach used to simulate climate.

Using a thermodynamic approach the author in the early sixties developed a time averaged model for predicting mean anomalies of the temperature, the precipitation and associated heating functions and circulations (Adem, 1962, 1963, 1964 *a*, 1964 *b*, 1965 *a*, 1965 *b*).

The basic idea behind the model is to use the thermodynamic energy equation applied to the atmosphere - ocean - continent system as the forecasting equations. The other equations are used diagnostically together with parameterizations for the

heating functions so that all the variables are expressed as functions of the surface temperature and the mean atmospheric temperature.

A second essential assumption is the use of an exchange coefficient of the order of  $3 \times 10^{10} \text{ cm}^2 \text{ sec}^{-1}$  for the horizontal turbulent transport of heat in the atmosphere and one of the order of  $3 \times 10^8 \text{ cm}^2 \text{ sec}^{-1}$  for the transport in the ocean.

Most of the previous applications of the model have dealt with the computation of anomalies of temperature, heating functions and circulations in the atmosphere and oceans for a period of a month, with the specific purpose of using the results for monthly weather prediction as well as for predicting ocean temperature anomalies for a month in advance (Adem, 1964 *a*, 1965 *b*, 1970 *a*, 1970 *b*, 1975).

Applications for paleoclimatic studies have been carried out by Shaw and Donn (1968, 1971) and Donn and Shaw (1975, 1977) who, using an earlier version of the present model, iterated it for several years, reaching a stable solution after the second year.

The effect of changing some of the climate parameters for a period of a month has been carried out by the author (Adem 1964 *a*, 1964 *b*, 1970 *b*, 1974). The present work is a direct extension of the above mentioned studies.

The purpose of the paper is to apply the latest version of the model in long term integrations, introducing a method for incorporating the change in the boundary of snow and ice as a variable, and iterating month by month the model several years until a stable solution is reached. The model will be applied to compute the effect on the climate of the Earth due to changes in the solar constant, and a comparison with computations made by other authors and with other models will be made.

### BRIEF DESCRIPTION OF THE MODEL

The model (Adem, 1964 *a*, 1965 *a*, 1965 *b*) is formed by an atmospheric layer of about 10 km high, which includes a cloud layer, an oceanic layer of 100 to 50 meters in depth and a continental layer of negligible depth. It also includes a layer of ice and snow over the continents and oceans.

It is postulated that the simplest possible realistic model of climate includes as the basic prognostic equations those of conservation of thermal energy applied to the atmosphere-ocean-continent system described above.

Time averaging of the variables of the order of a month is used; and it is assumed that the equations of hydrostatic equilibrium, perfect gas and the continuity

equation are valid for the time averaged variables.

As mentioned above, a constant horizontal diffusion coefficient is used both for the atmospheric layer and for the oceanic one.

The vertically integrated equation of thermal energy for the atmospheric layer is the following (Adem, 1965 *a*):

$$c_v a_0 \frac{\partial T'_m}{\partial t} + AD_1 - c_v a_0 K \nabla^2 T'_m - c_v K \mathbf{b} \cdot \nabla T'_m = E_T + G_5 + G_2 \quad (1)$$

where  $\nabla$  is the two-dimensional horizontal gradient operator;  $T'_m$  is the deviation of the mean atmospheric temperature from a constant value  $T_{m0}$ ,  $T_{m0} \gg T'_m$ ;  $c_v$  is the specific heat of air at constant volume;

$$a_0 = \int_0^H \rho_O^* dz \quad , \quad AD_1 = c_v M_a \cdot \nabla T'_m \quad ,$$

$$M_a = \int_0^H \rho_O^* \mathbf{v}_H^* dz \quad \text{and} \quad \mathbf{b} = \int_0^H \nabla \rho^* dz \quad ,$$

where  $H$  is the constant height of the model atmosphere and  $\rho^*$  is the density given by

$$\rho^* = \rho \left( 1 + \frac{\frac{g}{R\beta} - 1}{\frac{\beta(H-z)}{T_m} - \frac{\beta H/2}{T_m}} \right)$$

$T_m = T_{m0} + T'_m$ ,  $\rho$  is a fixed constant density at  $z = H$ ,  $\beta$  is the constant lapse rate used in the atmospheric layer,  $g$  is the acceleration of gravity,  $R$  is the gas constant,  $\mathbf{v}_H^*$  is the horizontal component of the wind,  $\rho_O^*$  is the value of  $\rho^*$  obtained by replacing  $T_m$  by  $T_{m0}$ ; and  $K$  is the horizontal Austausch coefficient for the atmosphere.

On the right side of eq. (1),  $E_T$  is the rate at which energy is added by radiation,  $G_2$  is the rate at which heat is added by vertical turbulent transport from the surface, and  $G_5$  is the rate at which heat is added by condensation of water vapor in the clouds.

On the left side,  $c_v a_0 \partial T'_m / \partial t$  is the local rate of change of thermal energy, and  $AD_1$  and  $c_v a_0 K \nabla^2 T'_m$  are the advections of thermal energy by the mean wind and by horizontal eddies, respectively. The term  $c_v K \mathbf{b} \cdot \nabla T'_m$  will be neglected.

The equation for the ocean layer (Adem, 1970a) is:

$$h \left( \frac{\partial T'_s}{\partial t} + \mathbf{v}_{sT} \cdot \nabla T'_s - K_s \nabla^2 T'_s \right) + W = \frac{1}{\rho_s c_s} (E_s - G_2 - G_3) \quad (2)$$

where  $T'_s = T_s - T_{s0}$  is the departure of the surface ocean temperature  $T_s$  from a constant value  $T_{s0}$ ,  $T_{s0} \gg T'_s$ ;  $\rho_s$  is a constant density and  $c_s$  is the specific heat;  $h$  is the depth of the layer;  $\mathbf{v}_{sT}$  is the horizontal velocity of the ocean currents;  $W$  is the vertical transport of heat at the bottom of the layer;  $K_s$  is the constant Austausch coefficient;  $E_s$  is the rate at which energy is added by radiation;  $G_2$  is the rate at which sensible heat is given off to the atmosphere by vertical turbulent transport; and  $G_3$  is the rate at which the heat is lost by evaporation. The term  $h \partial T'_s / \partial t$  is the local rate of change of thermal energy;  $h \mathbf{v}_{sT} \cdot \nabla T'_s$  and  $-h K_s \nabla^2 T'_s$  are the horizontal rates of transport of thermal energy by mean ocean currents and by turbulent eddies, respectively.

In the continents, eq. (2) reduces to:

$$0 = E_s - G_2 - G_3 \quad (2')$$

Using parameterizations for  $E_T$ ,  $E_s$ ,  $G_2$ ,  $G_3$ ,  $G_5$ ,  $AD_1$ ,  $\mathbf{v}_{sT}$  and  $W$  the different components that appear in (1) and (2) are expressed as functions of  $T_s$  and  $T_m$  and/or of their first and second derivative with respect to the map coordinates  $x$  and  $y$ ; and therefore the problem is reduced to solving two equations with two unknowns.

The parameterizations of the heating and transport components require the use of physical laws and conservation principles supplemented by observed data,

so that the formulas used are semi-empirical (Clapp *et al.*, 1965). The same parameterizations as in previous papers will be used (Adem, 1965*b*, 1970*a*, 1970*b*).

In the model used in this paper the following assumptions have been made:

(a) For the atmospheric layer a prescribed constant lapse is used, and the density at the top of the atmospheric layer is also a prescribed constant.

(b) In equation (2) the horizontal transports of heat by the mean ocean currents and by turbulent eddies are neglected, as well as the vertical transport at the bottom of the oceanic layer.

(c) In equation (1),  $\partial T'_m / \partial t$  is replaced by  $(T'_m - T'_{mp}) / \Delta t$ ; where  $T'_{mp}$  is the value of  $T'_m$  in the previous month and  $\Delta t$  is the time interval, taken as a month. Similarly,  $\partial T'_s / \partial t$  in equation (2) is replaced by  $(T'_s - T'_{sp}) / \Delta t$  where  $T'_{sp}$  is the value of  $T'_s$  in the previous month, and  $\Delta t$  is also taken as a month.

Using the assumptions (b) and (c) equation (2) becomes linear algebraic in  $T'_s$  and  $T'_m$ . Combining it with equation (1) yields the following elliptic differential equation:

$$K \nabla^2 T'_m + F'_1 \frac{\partial T'_m}{\partial x} + F''_1 \frac{\partial T'_m}{\partial y} + F'_1 T'_m = F_2 \quad (3)$$

where  $F'_1$ ,  $F''_1$ ,  $F'_1$  and  $F_2$  are known functions of the map coordinates  $x$  and  $y$ .

#### INCORPORATION OF THE SNOW AND ICE BOUNDARY AS A VARIABLE

The snow and ice boundary is generated in the model by using the computed  $-4.5^\circ \text{C}$  surface isotherm, so that any point with a surface temperature equal to or below  $-4.5^\circ \text{C}$  is defined as being covered by snow and ice.

This limit corresponds to the 50 % monthly frequency of snow on the ground obtained by Clapp (1967).

The method of generating the snow (and ice) boundary by coupling it to a computed surface isotherm was used by the author previously (Adem, 1965*b*).

The model is iterated with time steps of one month. The process includes seasonal variations of solar radiation. In each time step the normal surface albedo as given by Posey and Clapp (1964) is used initially as in the previous studies. The

predicted  $-4.5^{\circ}\text{C}$  surface isotherm is then used to compute the surface albedo. This internally generated albedo, together with the other parameters computed in the first step, is again used to compute the surface temperature (as well as the other variables). This adjustment process is repeated until the difference of the computed temperatures (and surface albedos) for two consecutive computations is zero. This condition is usually satisfied after four or five iterations, and implies that in the solution the internally generated snow (and ice) boundary, coupled to the  $-4.5^{\circ}\text{C}$  computed surface isotherm has also reached a stable location.

This iterative coupling between snow boundary and surface temperature is carried out for every time step both using the present solar constant and again using an anomaly in the solar constant. These two stages will be called for short the "normal case" and the "abnormal case". The rapid convergence of the solution is a manifestation of stability in the existing feedback. The presence of snow decreases the surface temperatures. On the other hand, the decrease of temperature to values lower than  $-4.5^{\circ}\text{C}$  perpetuates an existing snow cover.

To carry out the above process, we need to add two more fields to the ones already prescribed in the model: one of surface albedo without snow anywhere, and another with snow (and ice) over the entire Northern Hemisphere. Over the continents and oceans, the snow and ice boundary has been extended as far as the equator and the corresponding surface albedo has been estimated in order to obtain the second field. This simulates the effect of glaciation as far as the southernmost boundary of the present model.

Over the oceans, we assume that a surface albedo of 55 % corresponds to an ice-covered surface for temperatures lower than  $-4.5^{\circ}\text{C}$ . Over the continents, the best possible estimates of albedo have been used, based mainly on the work of Posey and Clapp (1964).

### TIME STEPS AND BOUNDARY CONDITIONS

In the experiments presented here the same approach will be followed as in previous papers, namely the normal case is computed first and then the abnormal one. However, the new aspect introduced in this paper is the adjustment of the snow boundary in each time step (month) both for the normal and the abnormal cases, and the iteration with monthly steps until an equilibrium steady state solution is reached.

The initial values for each time step are the mid-tropospheric temperature and the surface ocean temperature of the previous month.

Let the observed normal mid-tropospheric temperature and the observed normal surface temperature for the  $i^{\text{th}}$  month be designated respectively by the symbols  $T_{mN_{io}}$  and  $T_{sN_{io}}$ , and let  $T_{mN_i}$  and  $T_{sN_i}$  be the computed normal values, and  $T_{m_i}$  and  $T_{s_i}$  the corresponding computed abnormal values.

In the first step we use as initial values for both the normal and the abnormal cases the observed normal mid-tropospheric temperature ( $T_{mN_{io}}$ ) and the observed normal surface ocean temperature ( $T_{sN_{io}}$ ). The only difference in the first month for the normal and the abnormal cases is that in the first case we use the present normal insolation while in the abnormal case we use the same amount of insolation changed by a given percent.

For the subsequent steps, two alternatives or modifications of the initial conditions were used:

- 1)  $T_{mN_i}$  and  $T_{sN_i}$  for the normal case; and  $T_{m_i}$  and  $T_{s_i}$  for the abnormal one.
- 2)  $T_{mN_{io}}$  and  $T_{sN_{io}}$  for the normal case; and  $T_{mN_{io}} + (T_{m_i} - T_{mN_i})$  and  $T_{sN_{io}} + (T_{s_i} - T_{sN_i})$  for the abnormal one.

Parallel experiments using these two alternatives were carried out with a model with a fixed snow boundary, with the monthly surface albedo given by Posey and Clapp (1964).

In the case of the fixed snow boundary, both alternatives yielded the same anomalies. This is expected due to the linearity of the heating functions used in the model. However, the computed normals are much more realistic in the second alternative than in the first one.

Since the anomalies are the same for both cases, and realistic normal values are needed to generate realistic normal snow boundaries, the second modification of initial conditions was used in the experiments with the variable snow boundary model.

At the boundary of the integration region only anomalies due to radiation processes are generated and anomalies due to other processes are taken equal to zero. This can be done because the radiation function is a linear function of temperature, which allows the temperature anomaly to be computed algebraically. This anomaly can then be used to solve the elliptic differential equation (3) for the interior points of the integration region. Therefore, the boundary values vary through the integration.



The region of integration, the position of grid points and the method of integration used, will be the same as in previous papers (Adem, 1964a).

### CLIMATIC FLUCTUATIONS DUE TO A DECREASE OF TWO PERCENT IN THE SOLAR CONSTANT

The effect of decreasing the solar constant by two percent has been computed, using the model described above. The results are obtained as anomalies with respect to the present conditions.

Figure 1 shows the corresponding computed surface temperature change for January and July in tenths of Celsius degrees. In both cases, the anomalies are negative, and are stronger in July than in January.

The effect of the distribution of continents and oceans appears in the solution, especially in July. The largest anomalies are obtained in July over the continents, reaching values of  $-5.1$  degrees Celsius at latitude  $30^{\circ}$  over America and  $-6.0$  degrees at latitude  $20^{\circ}$  over Asia.

The solutions shown in figure 1 are obtained by starting the integration in the month of January and iterating several years with time steps of one month until the difference of the values for a given calendar month from one year to the next is less or equal to one tenth of a degree Celsius at every point of the integration region. A stable solution is obtained after 4 or 5 model years of integration.

Fig. 2 shows the profile of the solution for the surface temperature along the transpolar longitudes  $170^{\circ}$  W -  $10^{\circ}$  E, for different periods of integration.

The abscissa shows the latitude from the equator to the pole measured along  $170^{\circ}$  W, and then from the pole to the equator measured along  $10^{\circ}$  E. The ordinate shows ten times the negative of the anomaly of surface temperature. The first January month (short dashed line) has very weak anomalies, with values equal to or smaller than one tenth of a degree; except in the continents. After four months, in April (long dashed line), the anomalies increase to about 2 or 3 tenths of degrees Celsius in most regions, reaching values of about 3 or 4 tenth in the oceans and in the Antarctic, and 3 to 14 tenths in the continents. In July of the same first year (dotted line) the anomalies have values of 7 in the Pacific, 10 in the Arctic and increase from 7 to 26 tenths of degrees in the continents.

In October of the same first year of integration (continuous line) the values

are about the same as those of July in the Pacific, but are lower with respect to that month in the Arctic, where they are about 3; and have values of 5 in Europe and one in Africa.

In January of the second year, after thirteen one-month time steps (dotted dashed line), the anomalies are smaller than in July and October of the previous year, but larger than those for January of the previous year. The difference between the two Januaries is about 3 tenths of a degree in the Pacific and Arctic; and about 2 in Europe and Africa.

From figure 2, it is evident that the seasonal variations in insolation and snow cover are very important to the solution.

Figure 3 shows the negative of the anomalies of surface temperature for January along the same longitude line: for the first year, after one time step (dotted dashed line); for the second year after 13 time steps (short dashed line); for the third year after 25 time steps (heavy long dashed line); for the fourth year after 37 time steps (dotted line); for the fifth year after 49 time steps (continuous line). From this figure, it appears that the solution for January approaches asymptotically a steady state solution after about 4 years of integration with one-month time steps. Similar behaviour of the solution exists for the other months of the year.

It is of interest to point out that the anomalies corresponding to a 2 percent decrease of the solar constant for a time step of only one month (dotted dashed line) is considerably smaller than that obtained when the solution reaches the steady state solution (dotted line) after 4 years of integration. This remarkable difference is due mainly to the large heat storage capacity of the oceans, which tends to prolong the initial unperturbed conditions, and slows down the transition from the unperturbed to the perturbed conditions. The case in which the change in solar constant operates only during one month was treated previously by the author (Adem, 1974).

Besides the anomalies of surface temperature, other anomalies generated internally in the model are those of the mid-tropospheric temperature ( $T_m$ ), the snow and ice boundary, the heat of condensation of water vapor in the clouds ( $G_5$ ), the zonal and meridional components of the wind ( $u$  and  $v$  respectively), the horizontal advection of heat by the mean wind and by transient eddies ( $AD_1$  and  $TU_1$ , respectively), the heat added by short and long wave radiation at the surface and in the atmosphere ( $E_s$  and  $E_T$  respectively), the heat lost by evaporation at the surface ( $G_3$ ), the turbulent vertical transport of sensible heat from the surface to the atmosphere ( $G_2$ ), the horizontal extent of cloudiness ( $\epsilon$ ) and the storage of

heat in the oceans ( $ST_2$ ). In order to evaluate the complete effect of the decrease of solar constant in the earth's climate, the final equilibrium values of all the components of climate mentioned above should be studied.

Figure 4 shows the mid-tropospheric temperature change in tenths of Celsius degrees for January and July. In both cases, the anomalies are negative and larger in lower than in higher latitudes. In January, they vary from  $-1.5^{\circ}\text{C}$  in latitude  $15^{\circ}\text{N}$  to  $-0.6^{\circ}\text{C}$  at the North pole. The smallest value is  $-0.4^{\circ}\text{C}$  in Europe. In July, the negative anomalies vary from  $-1.7^{\circ}\text{C}$  at latitude  $15^{\circ}\text{N}$  to  $-1.0^{\circ}\text{C}$  at the North pole. The largest values are in the Atlantic near the Florida Peninsula ( $-2.3^{\circ}\text{C}$ ). The smallest value is  $-0.8^{\circ}\text{C}$  located at  $25^{\circ}\text{N}$ ,  $120^{\circ}\text{E}$ .

Figure 5 shows the change in the horizontal extent of cloud cover, in percent of the sky covered. The effect of the anomalies of cloud cover is especially important in the summer over the continents in latitudes below  $40^{\circ}\text{N}$ , where the surface temperature anomalies due to an increase in the anomalies of cloudiness reach values of about  $-5^{\circ}\text{C}$  (see figure 1).

The change in the heat of condensation of water vapor in the clouds for January is given (in langleys per day) by multiplying the corresponding values in figure 5 by 0.50; and for July by multiplying the corresponding values in figure 5 by 0.85. This change is proportional to that of precipitation. Therefore, these results show that a 2 % decrease in solar constant produces an increase in precipitation in January, except in higher latitudes and over an extensive region of Asia. In July, the effect is also to increase the precipitation, except in a large area of the North Pacific and North Atlantic, where there is a decrease. At the North pole and in the eastern part of the Mediterranean Sea, there is also a decrease of precipitation.

Due to limitation of space the figures showing the other components of climate cannot be presented here. However, some representative points, chosen arbitrarily, have been selected for which the values of the corresponding changes are given. Table 1 shows the values for points along the transpolar longitudes  $100^{\circ}\text{W}$  –  $80^{\circ}\text{E}$ , which, except for the pole, are continental points. Table 2 shows points in the Atlantic and Pacific oceans, and some points in continents far away from those of table 1 and representative of the behaviour of the solution.

From an analysis of tables 1 and 2 one can draw the following remarks:

1. The changes in  $G_2$ ,  $G_3$ ,  $E_s$  and  $E_T$  are larger in July than in January, and are, in general, negatively correlated with  $\epsilon$  (and  $G_5$ ), especially in July.

2. The change in the zonal wind ( $u$ ) is of the order of a few decimeters per second and it is an easterly wind over most of the integration area, with the largest values in lower latitudes. The change in the meridional wind ( $v$ ) is of the same order of magnitude than the zonal wind, with the largest values also in the lower latitudes.

3. The changes in the terms  $AD_1$  and  $TU_1$  are of an order of magnitude comparable to the other terms. The change in  $TU_1$  is positively correlated with the change in cloudiness ( $\epsilon$ ).

4. The change in  $ST_2$  is negative in July with most values from  $-5$  to  $-10$  langleys per day. In January the corresponding values are positive and equal to about 5 langleys per day.

5. From the above results it is evident that the solution depends in an important way on cloudiness.

In order to be able to compare some of the results with those obtained with zonally averaged models, the zonally averaged values for January, April, July and October, of the changes in surface temperature, and heat of condensation of water vapor in the clouds have been computed, and are shown in figures 6 and 7 respectively. The continuous lines are the values for January, the dotted lines for April, the dashed-dotted lines for July and the dashed lines for October. The anomalies of surface temperatures are always negative and increase towards lower latitudes. For a given latitude, the largest anomalies are in July and the smallest in January. At the surface, in January the values are about  $-1.6^\circ\text{C}$  from  $90^\circ\text{N}$  to  $40^\circ\text{N}$ , and increase to about  $-1.7^\circ\text{C}$  at latitude  $15^\circ\text{N}$ . In July they vary from  $-1.0^\circ\text{C}$  at latitude  $70^\circ\text{N}$  to  $-2.4^\circ\text{C}$  at latitude  $15^\circ\text{N}$ .

Figure 7 shows that the change of heat released by condensation of water vapor in the clouds is positive except for weak negative values in January from  $50^\circ\text{N}$  to  $90^\circ\text{N}$ ; in April from  $70^\circ\text{N}$  to  $90^\circ\text{N}$ ; in July from  $35^\circ\text{N}$  to  $50^\circ\text{N}$  and from  $70^\circ$  to  $90^\circ\text{N}$ ; and in October from  $63^\circ\text{N}$  to  $90^\circ\text{N}$ . The largest values are at lower latitudes, the maxima being 5 langleys per day in October, 4 in July and 3 in April, all at latitude  $15^\circ\text{N}$ ; while in January the maximum is 2 langleys per day at  $20^\circ\text{N}$ .

As pointed out above, the anomalies of the horizontal extent of cloudiness are directly proportional to the anomalies of heat of condensation, and are responsible for the large negative anomalies of temperature in lower latitudes.

Figure 8 shows the zonally averaged surface temperature change, for January

and July, corresponding to changes of the solar constant of  $+2\%$ ,  $-2\%$ ,  $-4\%$  and  $-10\%$ . The anomalies (with respect the present values) have the same sign as that of the anomalies of the solar constant. The absolute values of the anomalies are substantially larger in summer than in winter, and always increase towards lower latitudes.

The computed hemispheric average sea level temperature change due to the  $2\%$  decrease in solar constant is  $-1.0$  in January,  $-1.2$  in April,  $-1.7$  in July and  $-1.3$  in October, and the annual average is  $-1.3^{\circ}\text{C}$ . The change due to a decrease in  $1\%$  would be approximately half of these values. Therefore, one obtains in this case a change in the annual sea level temperature of about  $-0.7^{\circ}\text{C}$ .

### ANOMALIES OF SNOW AND ICE

A decrease of 2 percent in the solar constant produces anomalies in the extent of the snow boundary only during fall. For other seasons, no anomalies appear in the snow.

Figure 9 shows the case for October. The closed region around the pole is the snow cover generated with the present solar constant. The squares labeled II are those where there is an increase of snow due to a decrease of 2 percent in the solar constant, corresponding to the experiment described above.

It is interesting to study the evolution of the snow boundary when the solar constant continues to decrease. For this purpose, experiments were carried out with decreases in the solar constant of 4 percent and 10 percent.

The regions labeled IV in figure 9 are those where there were the additional increases in snow cover, besides those labeled II, and correspond to a decrease of 4 percent in the solar constant.

The regions labeled X are those with an additional increase in the snow cover, besides those labeled II and IV, and correspond to a decrease of 10 percent in the solar constant.

Using the same labeling for the snow covered areas, figure 10 shows the evolution of the snow boundary for January.

Figures 9 and 10 indicate that, for decreases of 2 to 4 %, no substantial displacement toward the south of the snow boundary occurs. With a decrease of 10 %, important anomalies of ice and snow appear. However, the additional snow

in winter and fall melts in summer, and does not produce a significantly different snow and ice regime than the present one.

### COMPARISON WITH RESULTS OF OTHER AUTHORS

Other models have been applied to estimate the effect of changes in the solar constant on the climate of the earth.

Sellers (1969, 1973) and Budyko (1969) using zonally averaged thermodynamic models found that a decrease of 1 % in solar radiation corresponds to a global decrease of 5° C in surface temperature, which is not in agreement with the 0.7° C decrease obtained in the present computations.

Due to the associated increase of ice cover, Sellers concluded that a decrease in solar constant by 2 to 5 % would be sufficient to initiate another ice age.

Similar results were obtained by Budyko who found that a comparatively small decrease of radiation - only 1.0 to 1.5 % - is sufficient for the development of ice cover on the land and oceans reaching south to temperate latitudes in the northern hemisphere. He also found that when radiation decreases by only 1.6 %, the ice cover reaches a mean latitude of about 50° N; after that, further decreases cause the snow line to start shifting rapidly towards lower latitudes down to the equator. At the same time, the planetary mean temperature drops sharply and reaches a value of several degrees below zero. On the other hand, the present results show that a decrease of 2 or 4 % in the solar constant does not produce a substantial increase in the position of the snow and ice boundary, and even a decrease as large as 10 % in the solar constant, which produces important anomalies in the ice covered regions of the Earth, does not produce a completely ice covered earth as obtained by Budyko with a much smaller decrease in solar radiation.

Wetherald and Manabe (1975) have also carried out computations to evaluate the effect of changing the solar constant using a simplified general circulation model, with a fixed cloud cover.

They also found that, contrary to Budyko's results, a decrease larger than 4 % is required to induce ice cap instability. They found, as in this study, that an increase (decrease) of the solar constant corresponds to an increase (decrease) of temperature. However, in contrast with the results of this paper, they found, as well as Budyko and Sellers, that the magnitude of the changes decreases toward lower latitudes.

They found that the annual average sea level temperature due to 1 % decrease of solar constant is of  $-2.1^{\circ}\text{C}$ .

Manabe and Wetherald (1967) applying a radiative-convective equilibrium model had computed earlier an annual average decrease in the surface temperature of  $-1.3^{\circ}\text{C}$  due to a 1 % decrease in the solar constant, and the same authors (Wetherald and Manabe, 1975) using a version of the Rodgers and Walstaw (1966) radiation model which was modified by Stone and Manabe (1968), found a corresponding decrease in surface temperature of  $-1.1^{\circ}\text{C}$ .

An interesting and novel approach is the one by Weare and Snell (1974) who proposed a diffuse thin cloud model structure, which couples the radiative properties of the atmosphere to the surface temperature providing considerable negative feedback. Application of this model to evaluate the change of surface temperature due to a change in solar constant, yielded a change in the mean surface temperature of  $-0.7^{\circ}\text{C}$ , corresponding to the 1 % decrease of the solar constant. This result is in agreement with the computed change using the model presented here.

Recently Temkin and Snell (1976) developed an annual, zonally averaged, steady-state hemispherical climatic model which incorporates the diffuse thin cloud tropospheric structure of Weare and Snell as a cloudiness feedback mechanism.

Application of this model to the effect of changing the solar constant yields a change of  $-1.0^{\circ}\text{C}$  in the mean surface temperature, corresponding to a one percent decrease in the solar constant.

In Table 3, a summary is given of the results by the different authors and models mentioned above, regarding the change in surface temperature due to a decrease of 1 % in the solar constant.

## FINAL REMARKS AND GENERAL CONCLUSIONS

From the analysis of tables 1 and 2 it is evident that it is essential to include cloudiness as a variable in any climate model, and in the case of the model used in these experiments a better parameterization of this variable is required.

The computations have shown that the zonally averaged values of the decrease of surface temperature due to a decrease of the solar constant is larger in lower than in higher latitudes. This is due to the inclusion of a variable cloud cover which

has a strong influence in the surface temperature decrease, especially in lower latitudes.

However, the boundary conditions which also vary through the integration and where only anomalies of radiation processes have been included (which also depend on the cloud anomalies) also determine to a large extent the values of the anomalies in lower latitudes.

The coupling of temperature with the snow-ice layer which is obtained with the procedure used in the model, described in section 3, is very weak. This is also one of the reasons of the relatively smaller changes of temperature in higher than in lower latitudes. Furthermore, Clapp (private communication), has pointed out to the author that the  $-4.5^{\circ}\text{C}$  isotherm used in the computations corresponds to the 50 % probability of snow only with light monthly precipitation amounts (0 to 1 inch); and that a better average for all precipitation amounts is  $-3.3^{\circ}\text{C}$  to  $-2.8^{\circ}\text{C}$ . Perhaps the choice of such a low temperature limit accounts for the rather small changes in our results when a variable snow boundary is introduced.

It has also been suggested by a reviewer that the use of the  $-4.5^{\circ}\text{C}$  to delineate ice cover over the oceans seems unrealistic, and that a value closer to  $0^{\circ}\text{C}$  would be preferable and might make a significant difference in the results.

Numerical experiments taking into account the above suggestions, as well as improved heating functions and a variety of boundary and initial conditions are now being carried out.

The purpose of this paper has been to show, as Shaw and Donn (1968, 1971) and Donn and Shaw (1975, 1977) have done already, the possibility of using this type of model, developed by the author for monthly predictions of temperature, in studies of climatic fluctuations.

It is evident from the results obtained above that the model presented here is a useful and fruitful alternative to other models for sensitivity studies of climate.

From the different results obtained as response of climate to changing the solar constant, it is clear that the answer to this question requires considerably more research, and the application of more realistic models, including the essential factors and processes in a correct way. The results reported here should therefore be considered of a very preliminary nature, and subject to possible improvements, when more advanced models become available.



## APPENDIX

*Parameterizations used in the author's thermodynamic model*

The parameterization of the rate at which energy is added by radiation in the atmosphere ( $E_T$ ) and at the surface ( $E_S$ ) is carried out assuming that the cloud layer and the surface of the Earth radiate as black bodies and that the clear atmosphere has a window for wave lengths between 8 and 13 microns (Adem, 1962).

Furthermore, the Savino-Ångström formula is used for the absorption of short wave radiation in the surface of the Earth.

The resultant formulas, linearized with respect to  $T_m$  and  $T_s$ , are of the type:

$$E_T = A_2'' T_m' + (A_3 + \epsilon D_3) T_s' + A_6 + \epsilon D_6' + (a_2 + \epsilon b_3) I \quad (A1)$$

$$E_S = B_2'' T_m' + B_3 T_s' + B_6 + \epsilon B_7 + \frac{(Q + q)_0}{I} [1 - (1 - k)\epsilon] (1 - \alpha) \quad (A2)$$

where  $A_2''$ ,  $A_3$ ,  $A_6$ ,  $D_3$ ,  $D_6'$ ,  $B_2''$ ,  $B_3$ ,  $B_6$ ,  $B_7$  are constants;  $\epsilon$  is the cloud cover;  $a_2$  and  $b_3$  functions of latitude and season;  $(Q + q)_0$  is the total radiation received by the surface with clear sky;  $k$  is a function of latitude;  $I$  is the insolation and  $\alpha$  the surface albedo (Adem, 1962, 1964a).

For the rates at which heat is added to the atmosphere by vertical turbulent transport from the surface ( $G_2$ ) and heat is lost by evaporation at the surface ( $G_3$ ), we use over the oceans the well known formulas:

$$G_2 = K_3 |v_a| (T_s - T_a) \quad (A3)$$

$$G_3 = K_4 |v_a| (0.981 e_s(T_s) - U e_s(T_a)) \quad (A4)$$

where  $K_4$  and  $K_3$  are constants,  $|v_a|$  is the ship-deck wind speed;  $T_a$  is the ship-deck air temperature;  $e_s(T_s)$  and  $e_s(T_a)$  are the saturation vapor pressure corresponding to the surface ocean temperature and the ship-deck air temperature, respectively; and  $U$  is the ship-deck air relative humidity.

Another alternative is the use of the linearized approximate formulas deduced by Clapp *et al.* (1965), adequate for use in the simpler linearized versions of the model, which are the following:

$$G_2 = G_{2N} + K_3 |v_{a_N}| [(T'_s - T'_{s_N}) - (T'_m - T'_{m_N})] \quad (A5)$$

$$G_3 = G_{3N} + K_4 B |v_{a_N}| [0.981 (T'_s - T'_{s_N}) - U_N(T'_m - T'_{m_N})] \quad (A6)$$

where  $G_{3N}$ ,  $G_{2N}$ ,  $T'_{s_N}$  and  $T'_{m_N}$  are the normal values of  $G_3$ ,  $G_2$ ,  $T'_s$  and  $T'_m$  respectively;  $B$  is a constant;  $U_N$  is the normal value of the surface relative humidity; and  $|v_{a_N}|$  is the normal surface wind speed.

In the continents we use for  $G_2$  a similar formula to that over the oceans and for  $G_3$  the formula

$$G_3 = G_{3N} + (1 - d_7)(E_s - E_{s_N}) \quad (A7)$$

where  $d_7$  is a seasonal value of the map coordinates and  $E_{s_N}$  is the normal value of  $E_s$  (Clapp *et al.*, 1965).

For the heat gained by condensation of water vapor in the clouds ( $G_5$ ), we use the following empirical formula deduced also by Clapp *et al.* (1965):

$$G_5 = G_{5N} + b(T'_m - T'_{m_N}) + d'' \left( \frac{\partial T'_m}{\partial x} - \frac{\partial T'_{m_N}}{\partial x} \right) + c'' \left( \frac{\partial T'_m}{\partial y} - \frac{\partial T'_{m_N}}{\partial y} \right) \quad (A8)$$

where  $G_{5N}$  is the normal seasonal value, and  $b$ ,  $d$  and  $c$  are functions of  $x$  and  $y$  that vary with the season.

For the horizontal wind we use the following formulas (Adem, 1970b):

$$u^* = - \frac{R}{fT} (T^* - (H - z) \frac{g}{R}) \frac{\partial T}{\partial y_1} \quad (A9)$$

$$v^* = \frac{R}{fT} (T^* - (H - z) \frac{g}{R}) \frac{\partial T}{\partial x_1} \quad (A10)$$

where  $u^*$  and  $v^*$  are the components along the  $x_1$  and  $y_1$  axes respectively of the horizontal wind, the  $x_1$  axis points to the east, the  $y_1$  axis to the north, and the vertical  $z$  axis upward;  $g$  is the acceleration of gravity,  $R$  the gas constant and  $f$  the Coriolis parameter;  $T = T_m - \beta H/2$  is the temperature at the top of the atmospheric layer, where  $\beta$  is the constant lapse rate used in the model; and  $T^* = T + \beta(H - Z)$  is the three dimensional temperature in the layer.

For the advection by mean wind ( $AD_1$ ) we use the formula (Adem, 1970*b*):

$$AD_1 = (F_8)_O J(T'_m, p_{N_{ob}}) + (F''_8)_O J(T'_m, T_{N_{ob}}) - (F'_8)_O J(T'_m, T'_{m_N}) \quad (A11)$$

where  $(F_8)_O$ ,  $(F''_8)_O$  and  $(F'_8)_O$  are constants; and

$$T_{N_{ob}} = -\beta(H - H_{7_{N_{ob}}}) + T_{7_{N_{ob}}}$$

$$p_{N_{ob}} = p_{7_{N_{ob}}} (T_{N_{ob}} - T_{7_{N_{ob}}})^{\frac{g}{R\beta}}$$

where  $H_{7_{N_{ob}}}$  is the normal observed 700 mb height,  $T_{7_{N_{ob}}}$  the normal observed 700 mb temperature and  $p_{7_{N_{ob}}}$  the 700 mb pressure.

The parameterization of the advection of heat by mean ocean currents is carried out using, for the total ocean current  $\mathbf{v}_{sT}$ , the formula

$$\mathbf{v}_{sT} = \mathbf{v}_{sw} + (\mathbf{v}_s - \mathbf{v}_{sN}) \quad (A12)$$

where  $\mathbf{v}_{sw}$  is the observed normal seasonal ocean current,  $\mathbf{v}_s$  is the pure wind drift current, and  $\mathbf{v}_{sN}$  is the corresponding normal wind drift current.

The components of the vector  $\mathbf{v}_s$  are computed from the following formulas:

$$u_s = c_1 \frac{0.0126}{\sqrt{\sin \varphi}} (u_a \cos \theta + v_a \sin \theta) \quad (\text{A13})$$

$$v_s = c_1 \frac{0.0126}{\sqrt{\sin \varphi}} (v_a \cos \theta - u_a \sin \theta) \quad (\text{A14})$$

where the directions of the coordinate axes are arbitrarily chosen;  $u_s$  and  $v_s$  are respectively the  $x$  and  $y$  components of the surface wind;  $\varphi$  is the latitude;  $c_1$  is a constant parameter, and  $\theta$  is the angle that measures the direction of the vector surface ocean current to the right of the surface wind direction. The detailed derivation of these formulas has been given elsewhere (Adem, 1970a) and is based on Ekman's formulas.

In the present model the upwelling term will be taken as zero.

The cloud cover is considered as a variable and is given by:

$$\epsilon = \epsilon_N + D_2 (G_5 - G_{5N}) \quad (\text{A15})$$

where  $\epsilon$  is the cloud cover,  $\epsilon_N$  the normal cloud cover and  $D_2$  is an empirical constant (Clapp *et al.*, 1965).

In the simplified version of the model used in the numerical experiments presented in this paper only formulas (A1), (A2), (A5), (A6), (A7), (A8), (A9), (A10), (A11) and (A15) have been used.

#### ACKNOWLEDGMENTS

The author is indebted to J. Zintzún from Centro de Ciencias de la Atmósfera, UNAM, for assisting him with the programming and with the numerical computations.

Climate component & Month	American Continent			North Pole	Asian Continent	
	100° W 20° N	100° W 35° N	100° W 60° N	90° N	80° E 50° N	80° E 25° N
$T_s$ July	-23	-50	-15	-12	-26	-20
	Jan.	-16	-9	-6	-7	-10
$T_m$ July	-16	-20	-11	-12	-10	-14
	Jan.	-12	-8	-7	-6	-15
$u$ July	-7	-2	0	0	0	-10
	Jan.	-10	-3	-1	-2	-7
$v$ July	-4	-4	0	0	0	0
	Jan.	0	0	0	-1	-1
$AD_1$ July	9	-2	0	0	0	0
	Jan.	10	-1	-1	-7	-5
$TU_1$ July	0	-3	0	-3	0	20
	Jan.	10	6	-2	5	-5
$\epsilon$ July	8	10	7	-1	6	20
	Jan.	10	3	-1	-1	-7
$G_5$ July	7	9	6	-1	5	17
	Jan.	5	2	-1	-1	-4
$G_2$ July	-10	-2	-3	0	0	-15
	Jan.	-3	-1	1	1	0
$G_3$ July	-3	-5	0	0	-4	-23
	Jan.	-10	-4	1	0	0
$ST_2$ July	0	0	0	0	0	0
	Jan.	0	0	0	0	0
$E_s$ July	-10	-7	-2	0	-5	-15
	Jan.	-8	-3	1	0	4
$E_T$ July	-5	-35	-5	-2	-15	-15
	Jan.	-5	-7	2	4	4

Table 1. Values, at representative points along the transpolar longitudes 100°W-80°E, of the changes of the components of climate, computed in the model, due to a 2 % decrease in the solar constant.  $T_s$  and  $T_m$  are in tenths of °C;  $u$  and  $v$  in decimeters per second;  $\epsilon$  in percent of cloud cover, and  $AD_1$ ,  $TU_1$ ,  $G_5$ ,  $G_2$ ,  $G_3$ ,  $ST_2$ ,  $E_s$  and  $E_T$  in Langley per day.

Climate component & Month		Atlantic Ocean		Pacific Ocean			Continent		
		65° W	45° W	130° W	180° W	130° E	105° E	20° E	20° E
		22° N	35° N	30° N	35° N	35° N	20° N	50° N	30° N
$T_s$	July	- 7	-10	-10	-12	- 7	-50	-14	-20
	Jan.	-10	- 7	-10	- 8	- 8	-15	- 4	- 7
$T_m$	July	-23	-17	-14	-16	-12	-11	-10	-12
	Jan.	-10	- 7	-10	- 8	- 9	-14	- 4	- 7
$u$	July	0	- 2	- 2	1	1	-10	- 1	- 5
	Jan.	- 8	- 2	- 2	2	- 2	- 5	0	- 3
$v$	July	0	- 2	1	0	- 5	10	0	0
	Jan.	1	0	0	0	2	1	0	0
$AD_1$	July	0	5	- 1	- 1	-14	10	0	- 4
	Jan.	5	- 3	- 1	- 1	10	1	0	- 3
$TU_1$	July	-50	-15	2	- 3	- 5	15	0	7
	Jan.	22	5	-10	5	7	- 1	4	10
$\epsilon$	July	-37	-13	- 3	- 2	0	60	5	5
	Jan.	10	2	5	2	5	2	0	5
$G_5$	July	-31	-11	- 3	- 2	0	51	4	4
	Jan.	5	1	3	1	3	1	0	3
$G_2$	July	45	15	6	10	15	-30	- 4	- 5
	Jan.	- 3	1	0	5	5	- 5	2	0
$G_3$	July	35	16	9	13	7	-30	- 1	3
	Jan.	-25	- 8	- 8	- 5	- 8	-10	0	-10
$ST_2$	July	- 5	- 9	-10	- 7	- 1	0	0	0
	Jan.	5	5	2	5	1	0	0	0
$E_s$	July	90	30	3	15	10	-18	-10	-10
	Jan.	-16	- 3	- 5	0	- 5	- 2	2	- 5
$E_T$	July	5	5	3	5	3	-25	- 5	- 5
	Jan.	- 2	- 1	- 2	0	- 3	0	0	- 5

Table 2. Values, at representative points in the Atlantic and Pacific oceans and at some points in continents far away from those of Table 1, of the changes of the components of Climate computed in the model, due to a 2 % decrease in the solar constant,  $T_s$  and  $T_m$  are in tenths of °C;  $u$  and  $v$  in decimeters per second;  $\epsilon$  in percent of cloud cover, and  $AD_1$ ,  $TU_1$ ,  $G_5$ ,  $G_2$ ,  $G_3$ ,  $ST_2$ ,  $E_s$  and  $E_T$  in Langleys per day.

Author	Year	Temperature change ( $^{\circ}\text{C}$ )	Type of model
Budyko	1969	- 5.0	Zonally averaged thermodynamic models with a vertically integrated layer for the atmosphere-surface of the earth system. Fixed cloudiness.
Sellers	1969, 1973	- 5.0	
Manabe & Wetherald	1967	- 1.3	Radiative-convective equilibrium model
Manabe & Wetherald	1975	- 1.1	Radiative - convective equilibrium model, using Rodgers-Walshaw radiation model, modified by Stone & Manabe
Manabe & Wetherald	1975	- 2.1	Simplified general Circulation Model. Fixed cloudiness.
Weare & Snell	1974	- 0.7	One - dimensional global model with diffuse cloudiness feedback.
Temkin & Snell	1976	- 1.0	Annual zonally averaged hemispheric model, with diffuse cloudiness feedback.
Adem	1978	- 0.7	Monthly hemispheric thermodynamic model. One layer for the atmosphere and one for the oceans and continents. The horizontal extent of cloudiness is a variable.

Table 3. Annual average sea level temperature change ( $^{\circ}\text{C}$ ) due to 1% decrease in the solar constant.

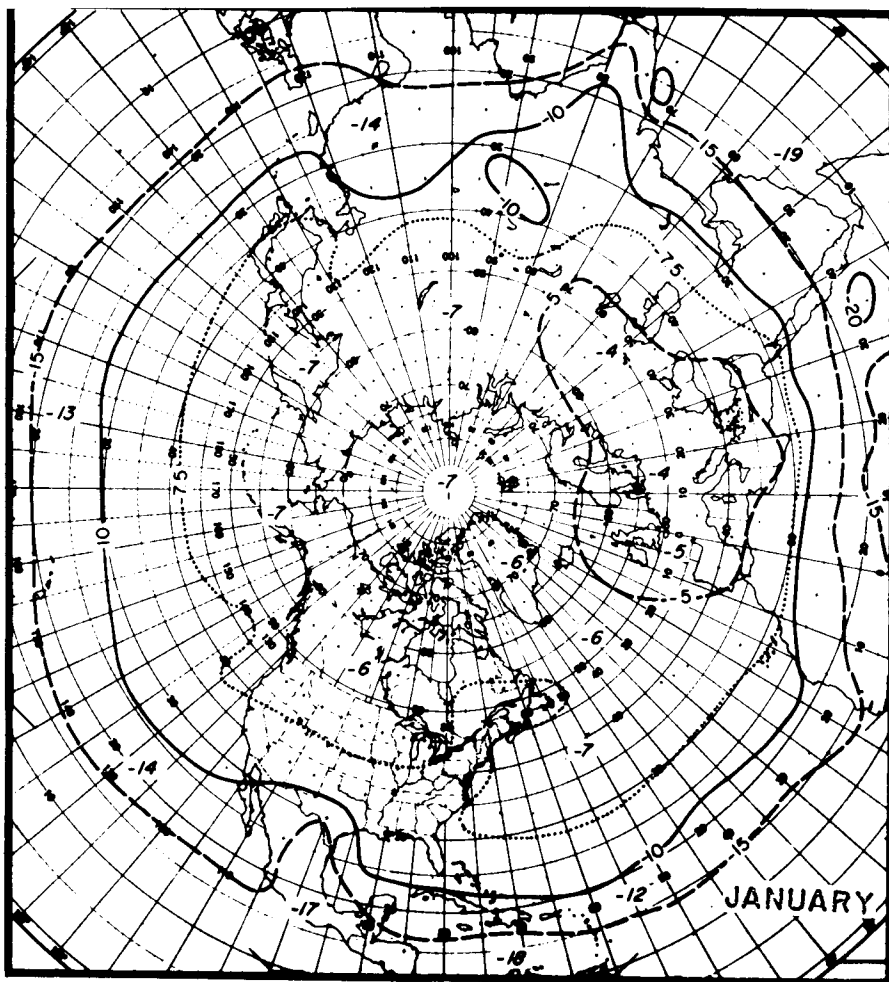
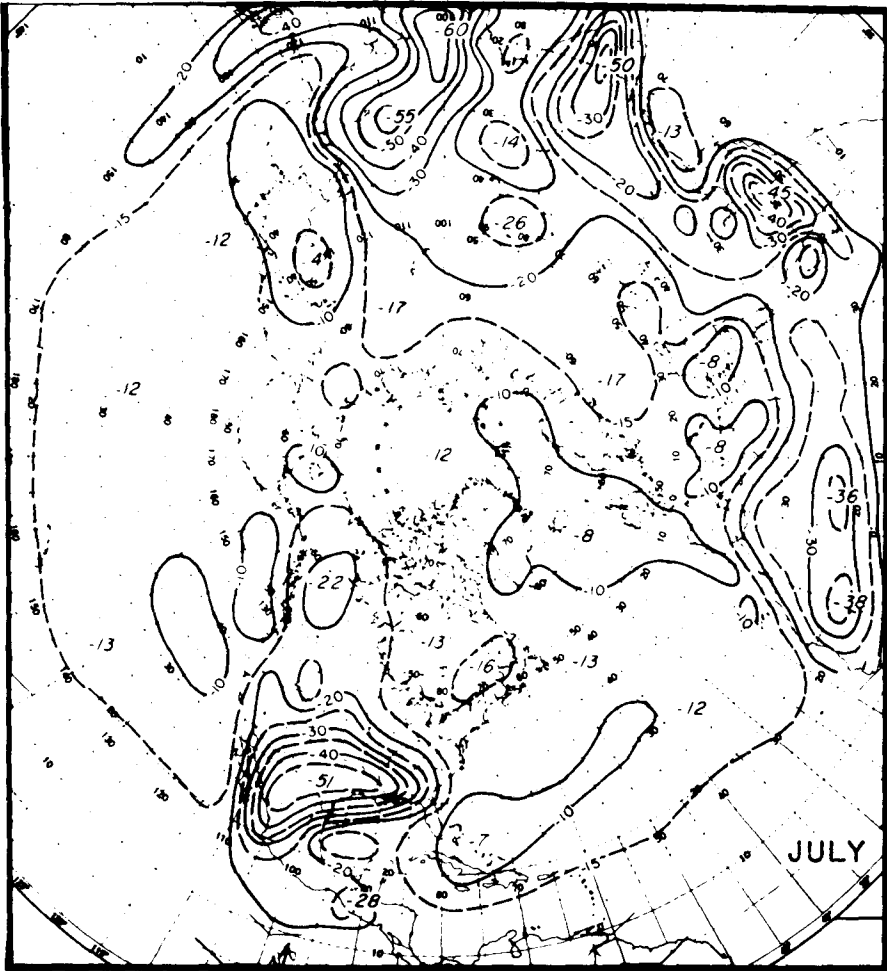


Fig. 1. Change in surface temperature, in tenths of Celsius degrees, for January and July, due to a decrease of 2 percent in the solar constant.





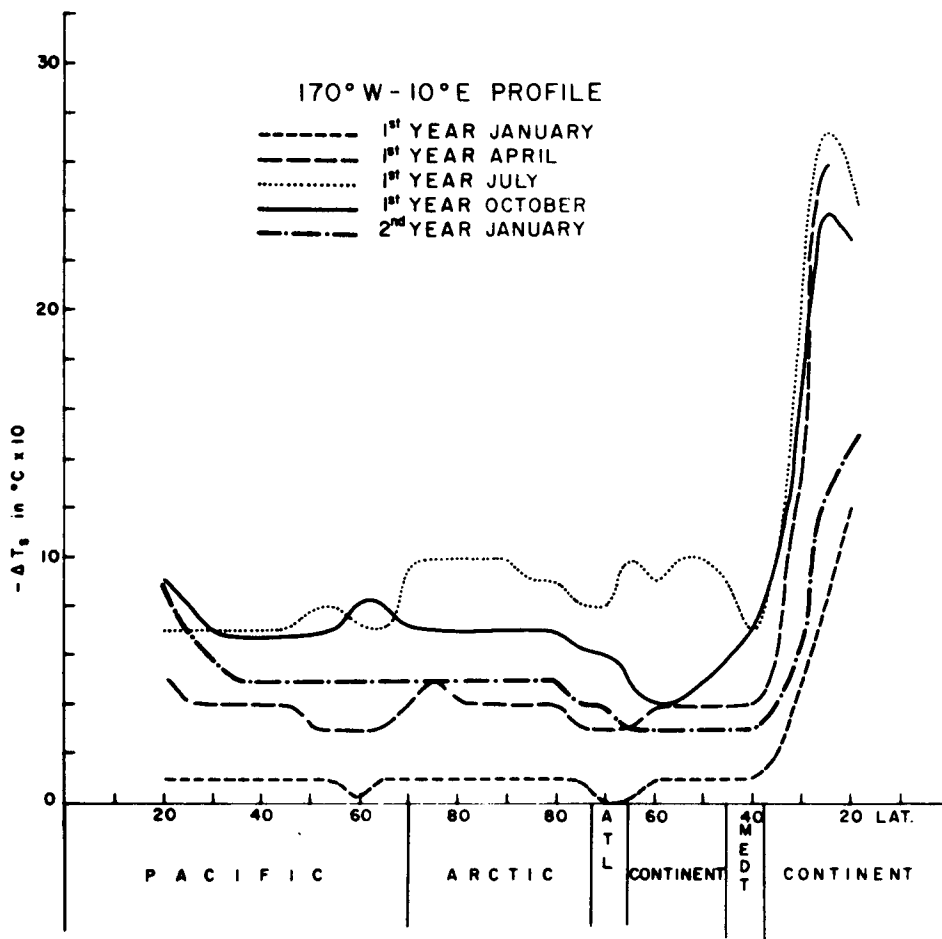


Fig. 2. The negative of the anomalies of surface temperature, in tenths of Celsius degrees, along the transpolar longitudes 170° W - 10° E, due to a decrease of two percent in the solar constant, for different periods of integration. The short dashed line represents the January values after a single time step of one month; the long dashed line, the April values after four months, the dotted line, the July values after seven months; the dotted line, the July values after seven months, the continuous line, the October values after ten months and the dotted-dashed line represents the January values after thirteen months.

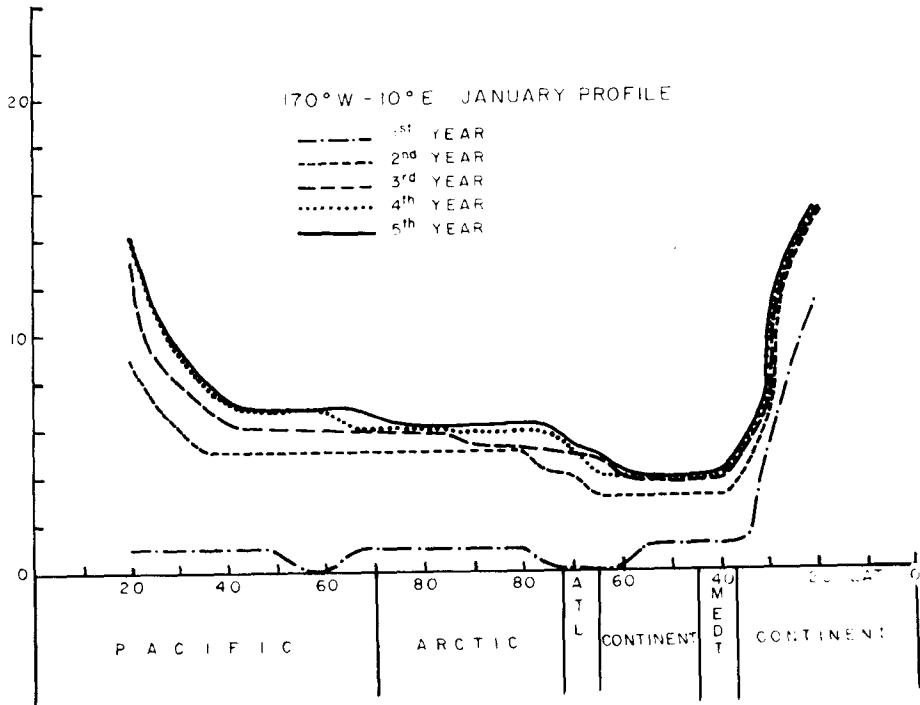


Fig. 3. The negative of the anomalies of surface temperature, in tenths of Celsius degrees, along the transpolar longitude  $170^{\circ} \text{W} - 10^{\circ} \text{E}$ , due to a decrease of two percent in the solar constant, for January and for different periods of integration. The dotted-dashed line represents the values after a single time step of one month; the short dashed line, the values after thirteen months; the long dashed line, after 25 months; the dotted line, after 37 months, and the continuous line represents the values after 49 months.

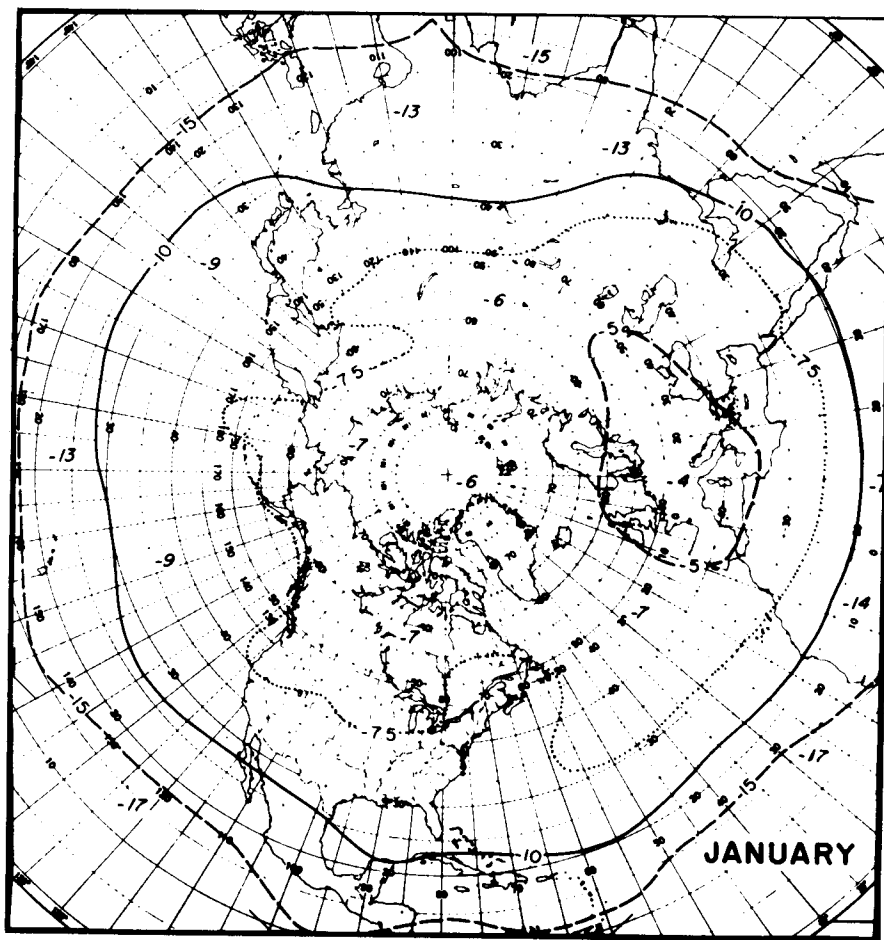
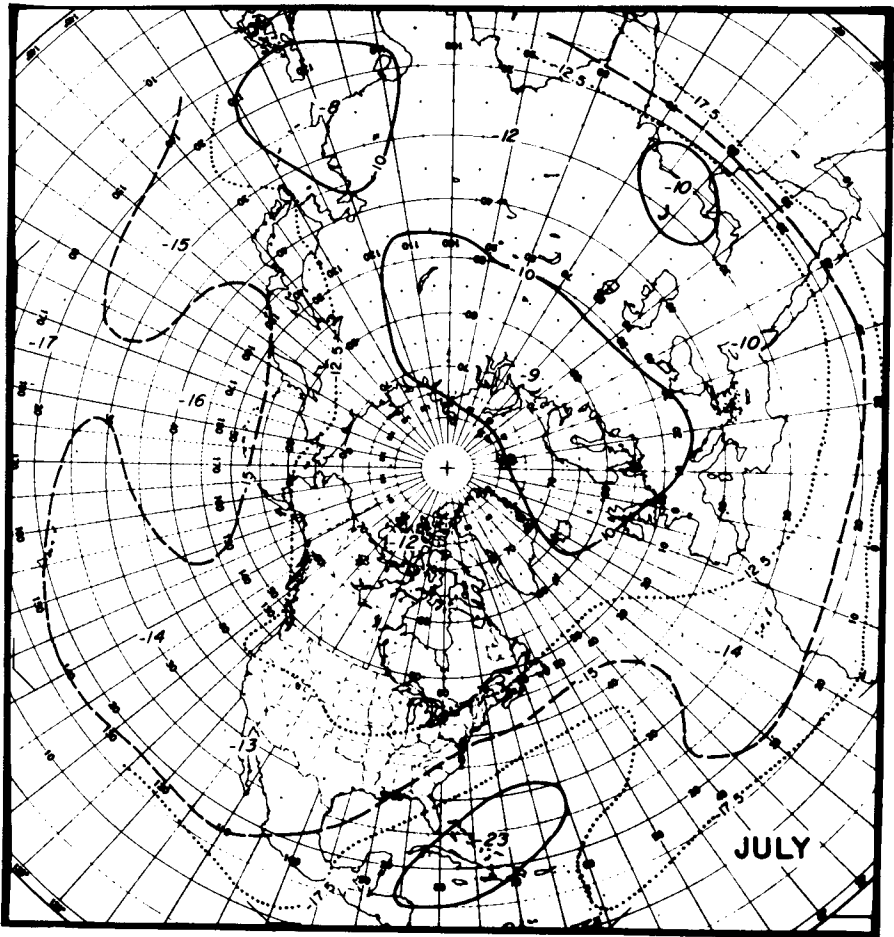


Fig. 4. Change in mid-tropospheric temperature in January and July, in tenths of Celsius degrees, due to a decrease of 2 percent in the solar constant.



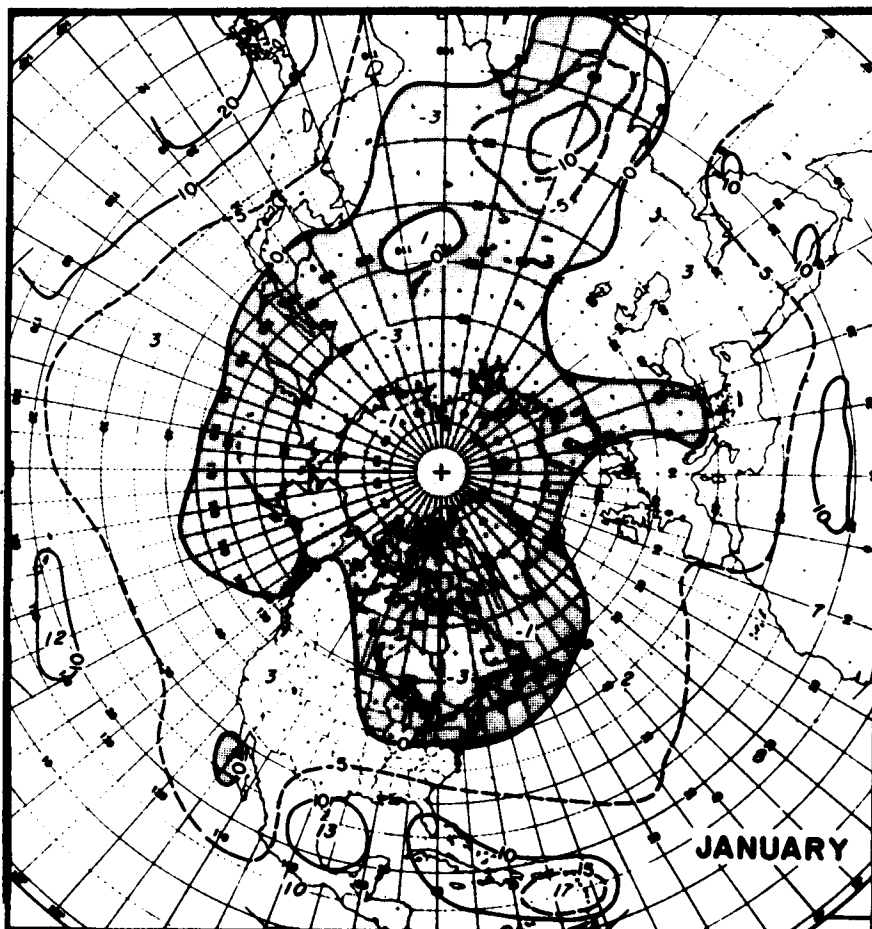
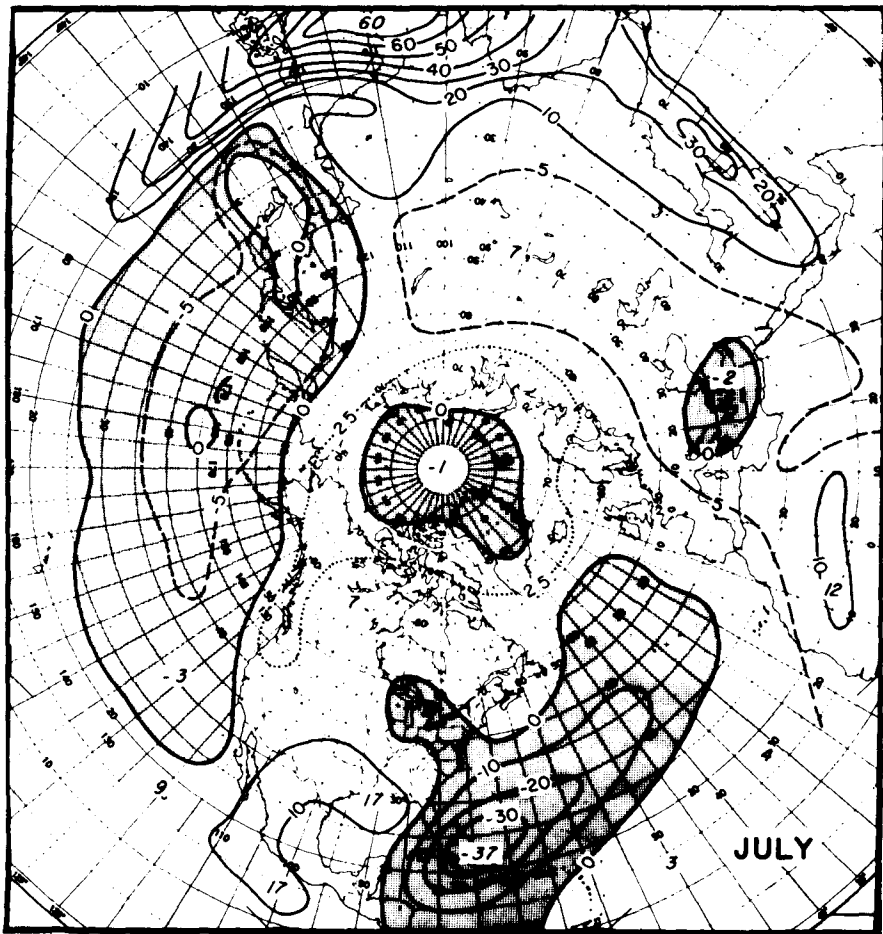


Fig. 5. Change in the cloud cover, in percent of the sky covered, for January and July due to a decrease of 2 percent in the solar constant. The change in the heat of condensation of water vapor in the clouds for January is given, in Langley's per day, by the cloud change values multiplied by 0.5; and for July by the corresponding values multiplied by 0.85.



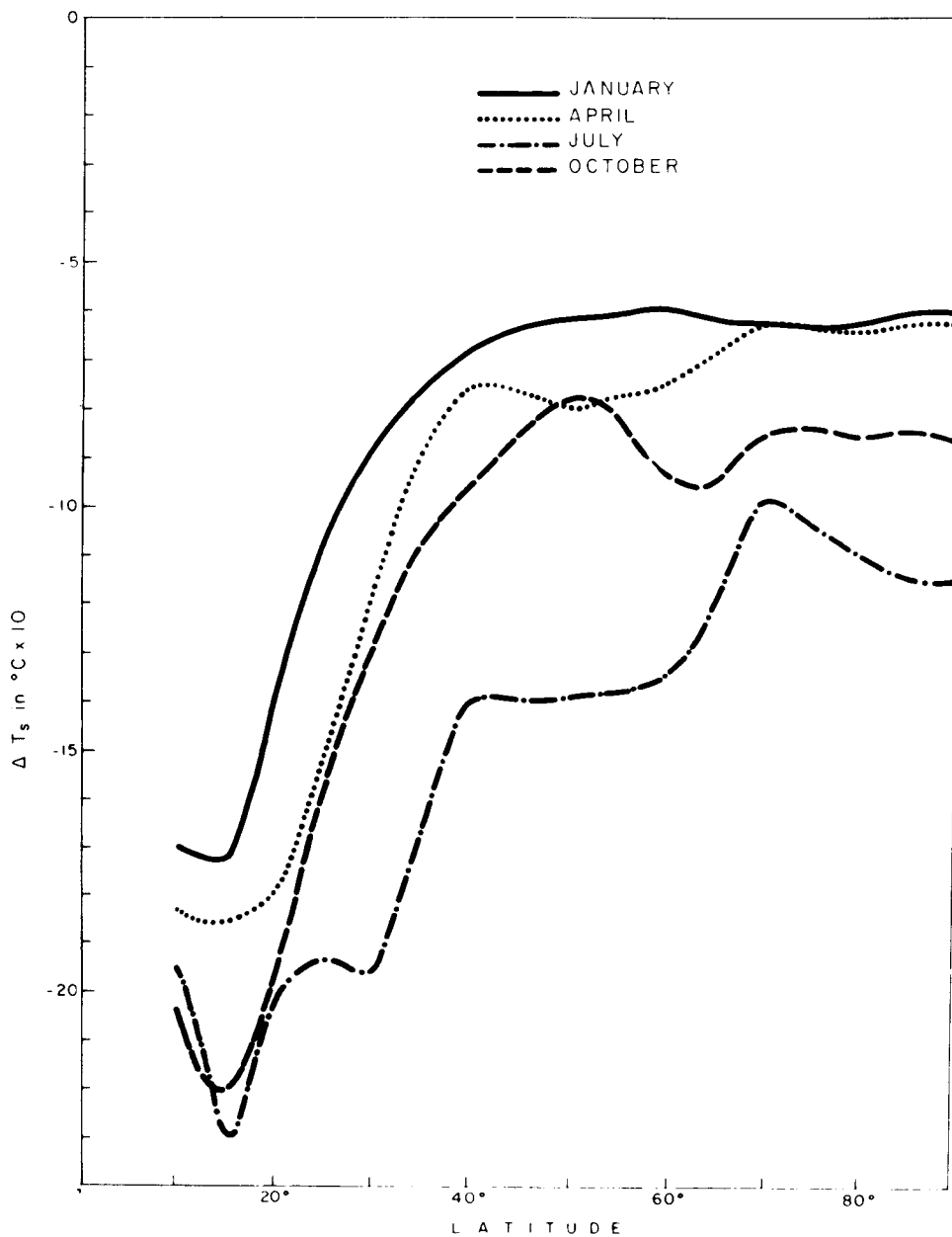


Fig. 6. Zonally averaged values of the change in the surface temperature, in tenths of degrees Celsius, due to a decrease of 2 percent in the solar constant.



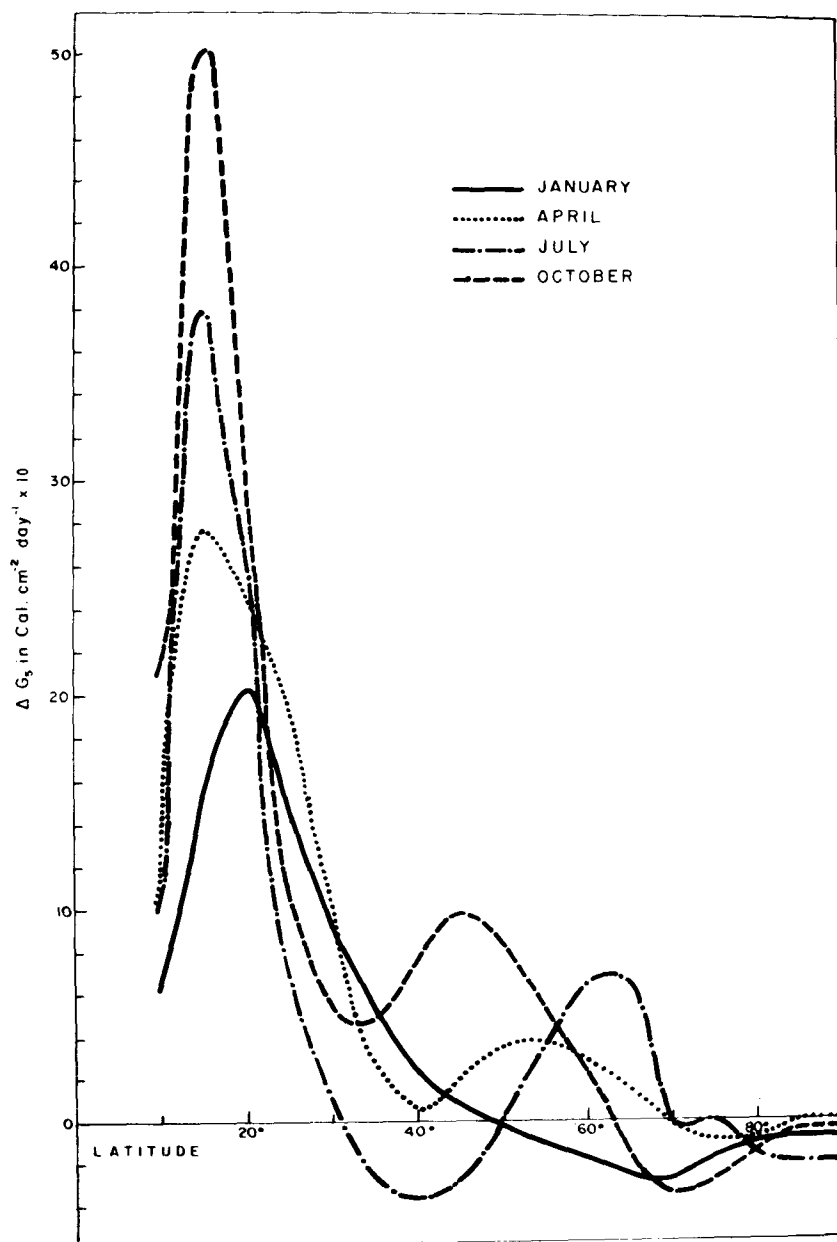


Fig. 7. Zonally averaged values of the change in the heat of condensation of water vapor in the clouds, in tenths of Langley's per day, due to a decrease of 2 percent in the solar constant.

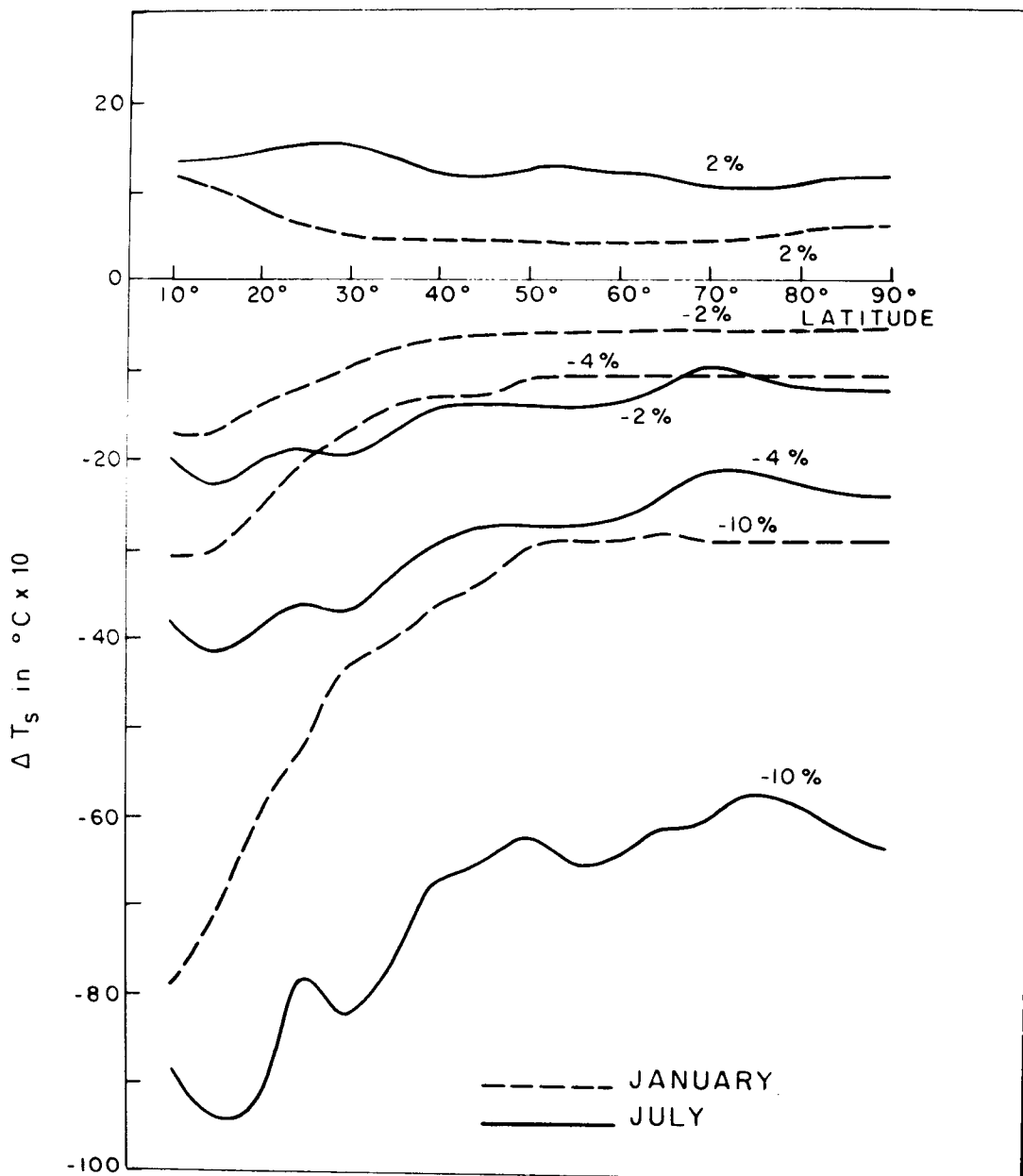


Fig. 8. Zonally averaged values of surface temperature change, in tenths of Celsius degrees, for January and July, corresponding to changes of the solar constant of +2, -2, -4 and -10 percent.

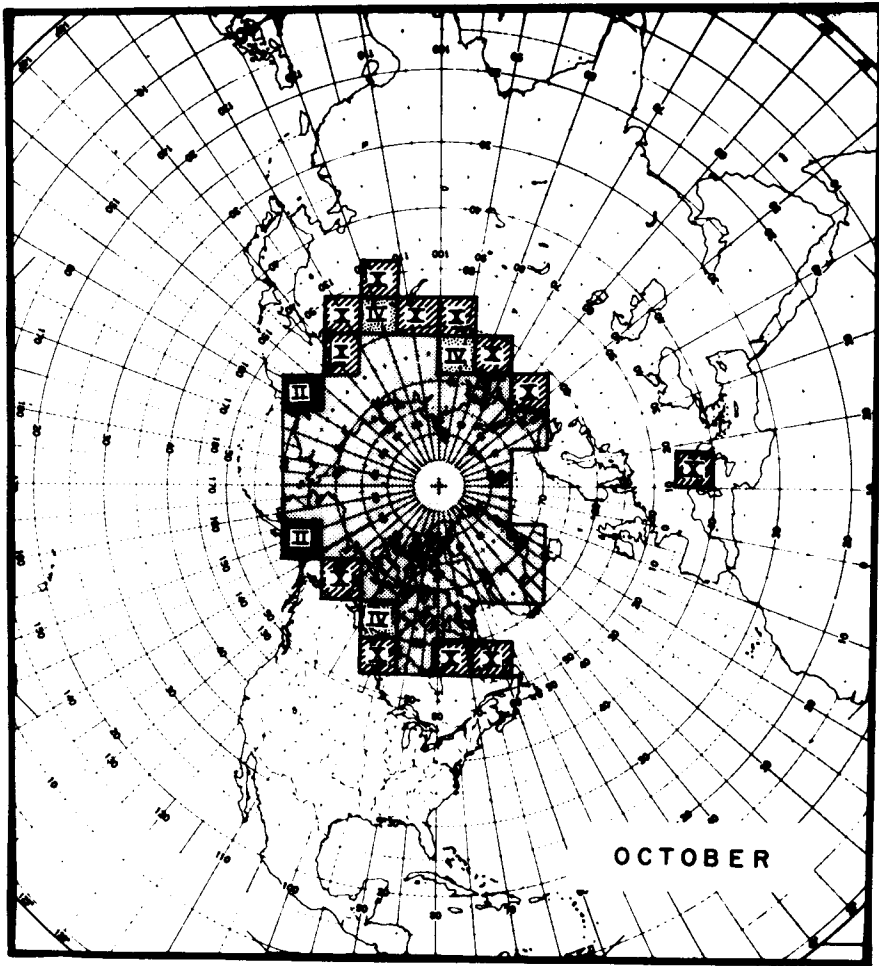


Fig. 9. Snow and ice cover generated by the model in October, for different values of the solar constant. The closed region around the pole corresponds to present normal conditions; the squares labeled II are the increases due to a decrease of 2 percent in the present value; those labeled II and IV are the increases due to a decrease of 4 percent; and those labeled II, IV and X are the increases due to a decrease of 10 percent.

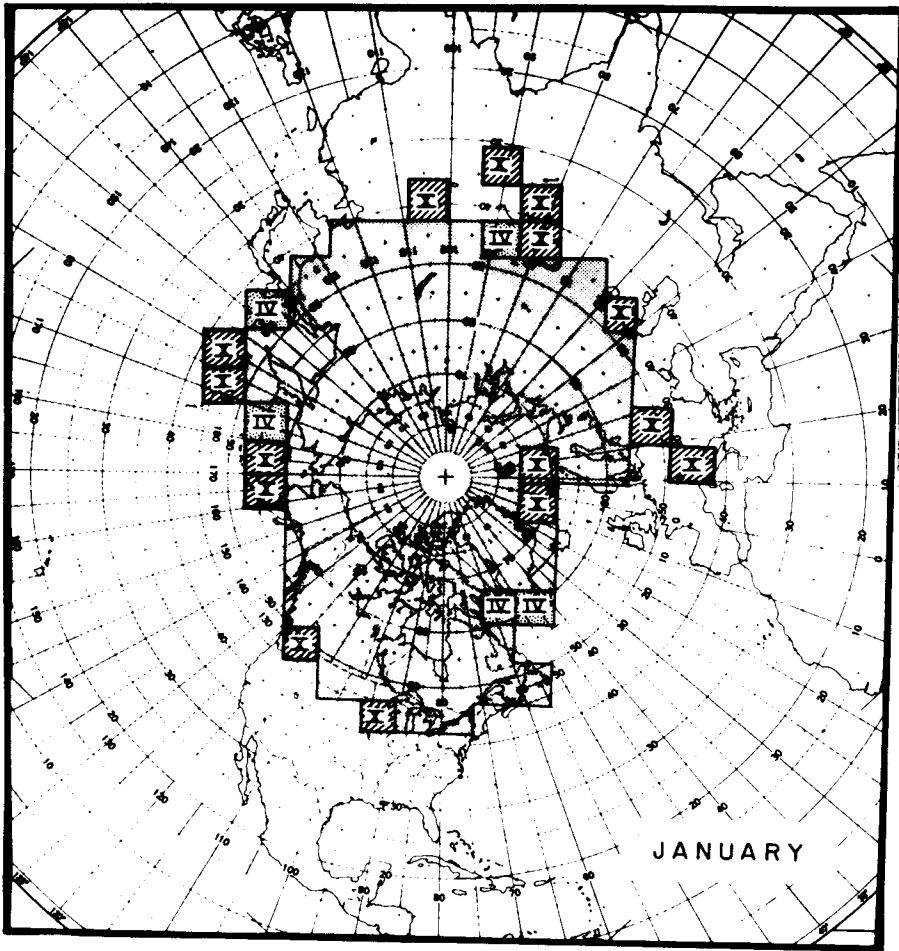


Fig. 10. Snow and ice cover generated by the model in January for different values of the solar constant. The closed region around the pole correspond to present normal conditions; the squares labeled IV are the increases due to a decrease of 4 percent in the present value; and those labeled IV and X are the increases due to a decrease of 10 percent.

## BIBLIOGRAPHY

- ADEM, J., 1962. On the theory of the general circulation of the atmosphere, *Tellus*, 14, 102-115.
- ADEM, J., 1963. Preliminary computations on the maintenance and prediction of seasonal temperatures in the troposphere. *Mon. Wea. Rev.* 91, 375-386.
- ADEM, J., 1964a. On the physical basis for the numerical prediction of monthly and seasonal temperatures in the troposphere-ocean-continent system. *Mon. Wea. Rev.*, 92, 91-104.
- ADEM, J., 1964b. On the thermal state of the troposphere-ocean-continent system in the Northern Hemisphere. *Geofis. Intern.*, 4, 3-32.
- ADEM, J., 1965a. Preliminary model for computing mid-tropospheric and surface temperatures from satellite data. *J. Geophys. Res.*, 70, 376-386.
- ADEM, J., 1965b. Experiments aiming at monthly and seasonal numerical weather prediction. *Mon. Wea. Rev.*, 93, 495-503.
- ADEM, J., 1970a. On the prediction of mean monthly ocean temperatures. *Tellus*, 22, 410-430.
- ADEM, J., 1970b. Incorporation of advection of heat by mean winds and by ocean currents in a thermodynamic model for long-range weather prediction. *Mon. Wea. Rev.*, 98, 776-786.
- ADEM, J., 1974. Thermodynamic approach for the study of climatic changes. Proceedings of the WMO Symposium on Physical and Dynamic Climatology. Leningrad, U.S.S.R., 1971, WMO. No.347, 359-389.
- ADEM, J., 1975. Numerical-thermodynamical prediction of mean-monthly ocean temperatures. *Tellus*, 27, 541-551.
- BUDYKO, M. I., 1969. Effect of solar radiation variations in the climate of the earth. *Tellus*, 21, 611-619.
- CLAPP, P. F., 1967. Specification of monthly frequency of snow cover based on macro-scale parameters. *J. of Appl. Meteor.*, 6, 1018-1024.
- CLAPP, P. F., S. H. SCOLNIK, R. E. TAUBENSEE and F. J. WINNINGHOFF, 1965. Parameterization of certain atmospheric heat sources and sinks for use in a numerical model for monthly and seasonal forecasting. Unpublished study of Extended Forecast Division. U. S. Weather Bureau, Washington, D. C., 20235.
- DONN, W. L. and D. M. SHAW. 1975. The evolution of climate. Proceedings of the WMO/IAMAP Symposium on long-term climatic fluctuations. Norwich, August 1975, WMO No. 421. XII, 503 pp.
- DONN, W. L. and D. M. SHAW, 1977. Model of climate evolution based on continental drift and polar wandering. *Geol. Soc. America Bull.*, 88, 390-396.
- MANABE, S. and R. T. WETHERALD, 1967. Thermal equilibrium of the atmosphere with a given distribution of relative humidity. *J. Atmos. Sci.*, 24, 241-259.

- POSEY, J. and P. F. CLAPP, 1964. Global distribution of normal surface albedo. *Geofis. Intern.* 4, 33-48.
- RODGERS, C. D. and D. C. WALSHAW, 1966. The computation of infrared cooling rate in planetary atmospheres. *Quart. J. Roy. Meteor. Soc.*, 92, 67-92.
- SELLERS, W. D., 1969. A global climatic model based on the energy balance of the earth-atmosphere system. *J. Appl. Meteor.*, 8, 392-400.
- SELLERS, W. D., 1973. A new global climatic model. *J. Appl. Meteor.*, 12, 241-254.
- SHAW, D. M. and W. L. DONN, 1968. Milankovitch radiation variations: A quantitative evaluation. *Science*, 162, 1270-1272.
- SHAW, D. M. and W. L. DONN, 1971. A thermodynamic study of arctic paleoclimatology. *Quaternary Res.*, 1, 175-187.
- STONE, H. M. and S. MANABE, 1968. Comparison among various numerical models designed for computing infrared cooling. *Mon. Wea. Rev.*, 96, 735-741.
- TEMKIN, R. L. and F. M. SNELL, 1976. An annual zonally averaged hemispherical climatic model with diffuse cloudiness feedback. *J. Atmos. Sci.*, 33, 1671-1685.
- WEARE, B. C. and F. M. SNELL, 1974. A diffuse thin cloud atmospheric structure as a feedback mechanism in global climatic modelling. *J. Atmos. Sci.*, 31, 1726-1734.
- WETHERALD, R. T. and S. MANABE, 1975. The effects of changing the solar constant on the climate of a general circulation model. *J. Atmos. Sci.* 32, 2044-2059.